Applied Physics Letters

Interface effects in nanometer-thick yttrium iron garnet films studied by magneto-optical spectroscopy

Cite as: Appl. Phys. Lett. **108**, 082403 (2016); https://doi.org/10.1063/1.4942379
Submitted: 11 November 2015 . Accepted: 06 February 2016 . Published Online: 23 February 2016

Eva Liskova Jakubisova, Stefan Visnovsky, Houchen Chang, and Mingzhong Wu

View Online Export Citation CrossMark

ARTICLES YOU MAY BE INTERESTED IN

Exquisite growth control and magnetic properties of yttrium iron garnet thin films
Applied Physics Letters **108**, 102403 (2016); https://doi.org/10.1063/1.4943210

Ferromagnetic resonance of sputtered yttrium iron garnet nanometer films
Journal of Applied Physics **115**, 17A501 (2014); https://doi.org/10.1063/1.4852135

Pulsed laser deposition of epitaxial yttrium iron garnet films with low Gilbert damping and bulk-like magnetization
APL Materials **2**, 106102 (2014); https://doi.org/10.1063/1.4896936

© 2016 AIP Publishing LLC.

Interface effects in nanometer-thick yttrium iron garnet films studied by magneto-optical spectroscopy

Eva Liskova Jakubisova,[1,a)] Stefan Visnovsky,[1] Houchen Chang,[2] and Mingzhong Wu[2]
[1]*Faculty of Mathematics and Physics, Charles University, Ke Karlovu 3, 12116 Prague, Czech Republic*
[2]*Department of Physics, Colorado State University, Fort Collins, Colorado 80523, USA*

(Received 11 November 2015; accepted 6 February 2016; published online 23 February 2016)

The properties of nanometer-thick yttrium iron garnet (YIG) films are strongly influenced by interfaces. This work employs spectral ellipsometry (SE) and magneto-optic polar Kerr rotation (PKR) to characterize YIG films with thickness, t, from 6 nm to 30 nm grown on $Gd_3Ga_5O_{12}$ (GGG) substrates oriented parallel to (111) plane. The films display a surface roughness of 0.35 nm or lower. The analysis of the SE data at the photon energies of $1\,eV < E < 6.5\,eV$ provided the t and permittivity values. The PKR at $1.3\,eV < E < 4.5\,eV$ is reasonably explained with the optical model for the YIG film/GGG substrate system. Even better agreement is achieved by assuming a 1.07-nm-thick layer sandwiched between YIG and GGG that has Fe^{3+} sublattice magnetization opposite to that in the YIG volume. This suggests the existence of antiferromagnetic coupling between the Gd^{3+} and tetrahedral Fe^{3+}. © *2016 AIP Publishing LLC*. [http://dx.doi.org/10.1063/1.4942379]

Low damping sub-100 nm thick yttrium iron garnet ($Y_3Fe_5O_{12}$, YIG) films present interest for miniaturized magnonic devices.[1–7] Chang *et al.*[8] reported high-quality YIG films deposited by magnetron sputtering on single-crystal $Gd_3Ga_5O_{12}$ (GGG) substrates and treated by annealing at 800 °C in O_2. Their films displayed the saturation magnetization $4\pi M_s$ values consistent with that in bulk YIG materials, sub-nm surface roughness, and very low damping with the Gilbert damping constant $\alpha = (8.58 \pm 0.21) \times 10^{-5}$. Recently, the properties of nm-thick YIG films were also characterized by spectral ellipsometry (SE) and magneto-optical (MO) polar Kerr effect (PKR) measurements.[9] The SE studies provided a refined information on the film thickness (t). The diagonal optical permittivity, the MO spectra, and the MO saturation magnetic field agreed with the data found for high-purity bulk YIG single crystals. The well resolved structure in the MO spectra indicated the absence of Fe cations other than Fe^{3+} as expected in the low damping films. The present work employs SE and MO PKR techniques to characterize the YIG films in the 6–30 nm thickness range with a focus on the roles of the YIG/GGG and air/YIG interfaces, as at the thickness $t \leq 10$ nm, the YIG film properties can be strongly influenced by these interfaces. There were several previous studies on interface effects in YIG films,[7,10–16] but no special attentions were devoted to sputtered, nm-thick, low-damping YIG films. Recently, Mitra *et al.* reported on thickness dependent magnetization in sputtered nanometer thick YIG film on (111) oriented GGG.[17]

The YIG films studied in the present work were prepared by sputtering on GGG substrates. Their thicknesses ranged from 6 nm to 26 nm. The details of the preparation process and microstructural characterization of the films were provided in Ref. 8. In brief, the sputtering process was carried out in Ar atmosphere with a sputtering power of 75 W onto (111)-oriented, one side polished, 0.5-mm-thick GGG substrates. After sputtering, the films were annealed at 800 °C in 1.1 Torr O_2 atmosphere for 4 h and then slowly cooled down (1 °C/min). The rms roughness of the film surface was determined by atomic force microscopy (AFM) measurements carried out in a tapping mode. The AFM images of investigated films (Fig. 1) showed the YIG film surface roughness of 0.35 nm or lower.

The films were studied by SE and MO azimuth rotation measurements in magnetic fields applied perpendicular to the sample planes. The GGG substrates had unpolished mat back faces, which helped increase the signal-to-noise ratio. To minimize the effect of spurious reflections, their back faces were painted with a non-reflecting black color before being fixed on the top of a water cooled pole piece. The pole was kept at a constant temperature of 12 °C. The SE data for the YIG/GGG samples and a bare GGG substrate were acquired using a Woolam variable angle spectroscopic ellipsometer at the angles of incidence between 55° and 70° in the photon energy range of $E = 1 - 6.5$ eV.

The PKR spectra were measured by the use of a MO spectrometer based on an azimuthal modulation technique using the following optical element sequence: 450W Xe arc lamp – quartz prism monochromator – polarizer – dc Faraday-rotation compensator – ac Faraday-rotation modulator – sample – analyzer – photomultiplier. The magnetic field was applied perpendicular to the sample surface (MO polar Kerr effect). The strength of the magnetic field was 5 kOe, which was more than sufficient to saturate the YIG films. The angle of light incidence is less than 10°. The spectra were measured in the energy range of $1.2\,eV < E < 4.5\,eV$. Further PKR measurements were carried out at a fixed radiation wavelength of 308 nm ($E \approx 4$ eV) as a function of the magnetic field, which was swept between −3 kOe and +3 kOe.

The numerical analysis of the SE data at the photon energy range of $1\,eV < E < 6.5\,eV$ assumed a YIG film sandwiched between an ambient and a GGG substrate, as shown in Fig. 2(a). The procedure provided optical constants for the

a)Author to whom correspondence should be addressed. Electronic mail: liskova@karlov.mff.cuni.cz

 © 2016 AIP Publishing LLC

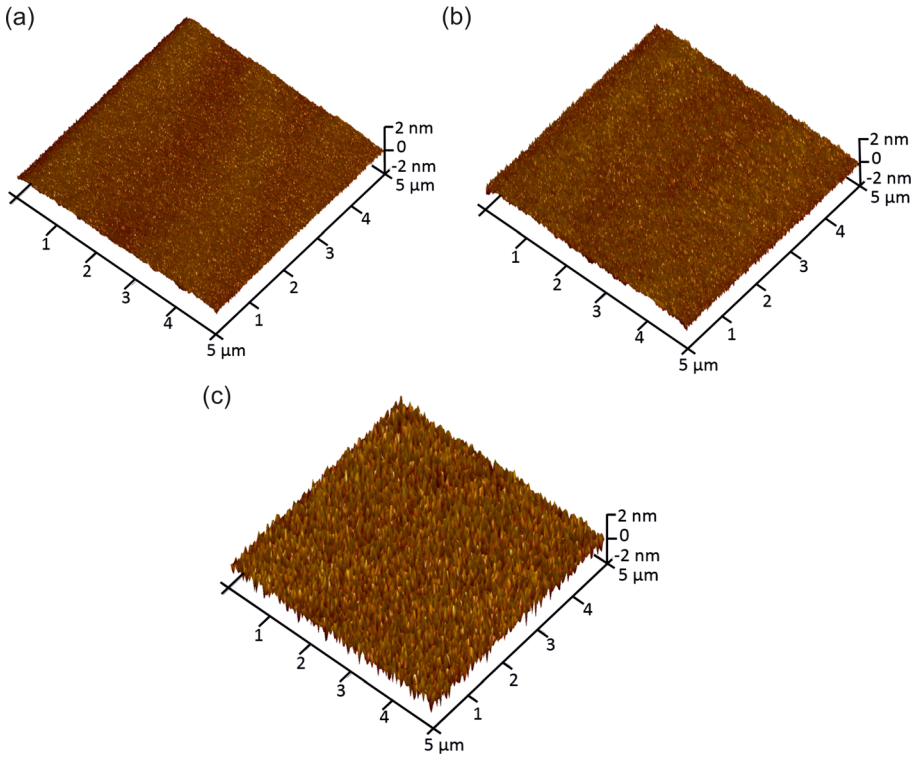

FIG. 1. AFM surface images of $Y_3Fe_5O_{12}$ films. (a) YIG26, (b) YIG20, and (c) YIG6. The details of these samples are provided in Table I.

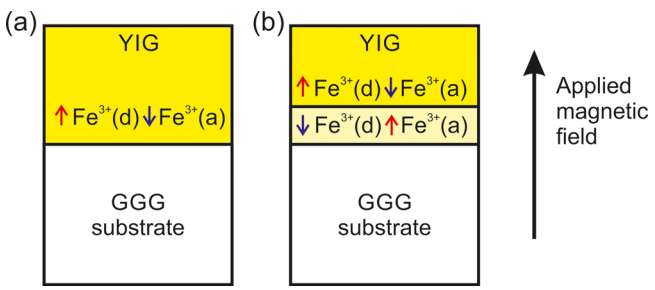

FIG. 2. Uniform yttrium iron garnet (YIG) film on gadollinium gallium garnet (GGG) substrate (a). YIG/GGG system with a region of reversed iron sublattice magnetization formed at the YIG–GGG interface (b). The magnetic field is applied normal to the film surface. Its orientation is indicated by an arrow on right. Under its action tetrahedral $Fe^{3+}(d)$ and octahedral $Fe^{3+}(a)$ spins order as shown.

YIG films, which are consistent with those expected for bulk YIG single crystals[9] and t values, which are close to the values estimated according to the growth rate and the sputtering time. The effects of the surface (air/YIG) and interface (YIG/GGG) roughnesses on the SE were negligible. The values of the nominal film thickness, the film thickness refined using SE, and the AFM-deduced surface roughness are given in Table I. The spectra of real index of refraction, n, and extinction coefficient, k, for the GGG substrate, which were required in the analysis of the data obtained for the YIG films, were determined from a separate SE experiment on a 0.5-mm-thick, (111)-oriented GGG substrate with one side polished. The results shown in Fig. 3 extend to higher E than those previously published.[18]

TABLE I. Characteristics of $Y_3Fe_5O_{12}$ films grown on (111)-oriented $Gd_3Ga_5O_{12}$ substrates.

Sample	YIG6	YIG12[a]	YIG20	YIG26
Nominal thickness (nm)	5		23	30
SE thickness (nm)	6.2	12	20.6	26.3
Surface roughness (nm)	0.35		0.14	0.088
Saturation field (kOe)	1.6	1.8	1.8	1.8

[a]Reference 9.

Figure 4 shows the PKR hysteresis loops (normalized to unity) measured with the magnetic field applied parallel to the crystallographic axis ⟨111⟩, the easy axis of the magnetocrystalline anisotropy. Note that the YIG films are all (111) oriented. In thicker films ($t \geq 12$ nm), the PKR hysteresis loops measured at a fixed radiation wavelength saturate in the field of about 1.8 kOe, which is close to the saturation magnetization in bulk YIG materials ($4\pi M_s = 1.75$ kG). For the thinnest film ($t \approx 6$ nm), the saturation field decreased to 1.6 kG, see Table I. The dominant contribution to the saturation field H_{sat} comes from the magnetic shape anisotropy, namely, $H_{sat} \approx 4\pi M_s$. Other contributions to H_{sat} originating

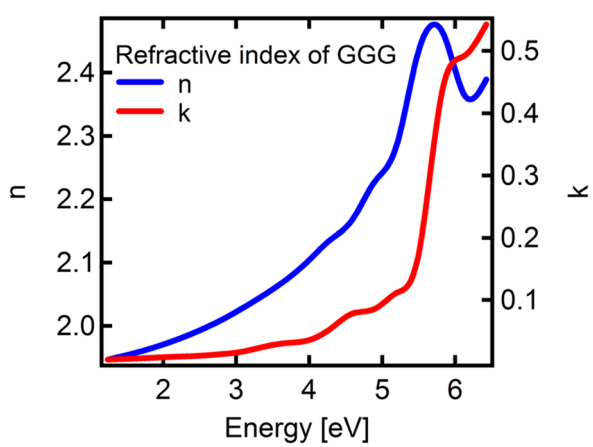

FIG. 3. Real index of refraction, n, and extinction coefficient, k, for $Gd_3Ga_5O_{12}$ measured on a (111) face.

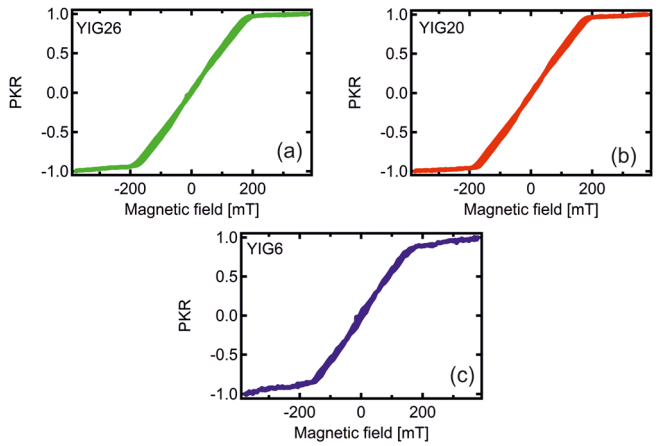

FIG. 4. Polar Kerr rotation (PKR) hysteresis loops (in arbitrary units) for samples YIG26 (a), YIG20 (b), and YIG6 (c), measured with the magnetic field applied parallel to the crystallographic axis ⟨111⟩ normal to the film plane at the photon energy of 4 eV.

from the magnetocrystalline anisotropy,[19] interface stress-induced magnetic anisotropies, and that due to a partial ($\approx 1\%$) Y^{3+} occupation of octahedral sites were assumed small and neglected. Figure 5 presents the measured PKR spectra for the YIG film samples. As the samples showed negligible MO rotations ($<0.005°$) at $E < 2.2$ eV, the range of displayed E was limited to 2.2–4.5 eV.

The optical permittivity spectra for YIG yielded from the analysis of the SE data are consistent with the results found for bulk YIG single crystals and epitaxial YIG films and also for nm-thick YIG films sputtered on GGG substrates assuming a simple film substrate system shown in Fig. 2(a).[9,20] The SE and PKR results confirm that the films are stoichiometric, have no Fe^{2+}, and preserve bulk YIG properties down to $t \approx 6$ nm. The computed PKR spectra in the samples employed the off-diagonal tensor elements of bulk YIG materials along with the optical constants for YIG[9] and GGG[18] materials shown in Fig. 3. The model[21] based on the system of Fig. 2(a) also reasonably reproduced the PKR

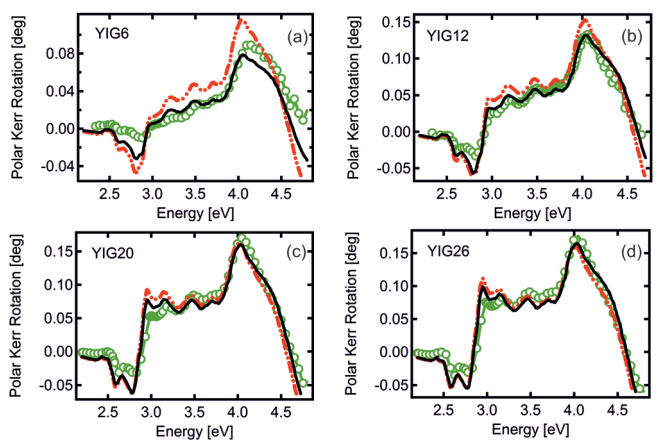

FIG. 5. Magneto-optic polar Kerr rotation spectra in nm-thick films of $Y_3Fe_5O_{12}$ deposited on (111)-oriented $Gd_3Ga_5O_{12}$ substrates. The green symbols show the experimental data. The curves represent the computed spectra using the data for bulk $Y_3Fe_5O_{12}$ and $Gd_3Ga_5O_{12}$ materials for the films of uniform magnetization (red dashed-dotted curves) and for the films with a 1.07-nm-thick interface layer with opposite orientations of Fe^{3+} sublattices (black curves).

structure but with somewhat higher computed amplitudes. In view of a significant ratio of interface to inner volume YIG unit cells in the films with $t \leq 30$ nm, the smaller amplitudes observed can be assigned to the manifestation of interface effects.

At first, an attempt was made to assign the reduced MO activity to the effects originating from the interface regions with either voids or mixing. However, the effective medium approach applied to both the air/YIG and YIG/GGG interface layers of varying thickness gave poor improvement.[22] This indicates that in the films with a sub-nm roughness and a very low defect concentration (leading to the low damping constant), there is no significant migration of Fe^{3+} and Ga^{3+} across the interface.[23] The SE data, indeed, confirmed negligible contributions from imperfections at the air/YIG and YIG/GGG interfaces, which is consistent with the sub-nm surface roughness. As the structure in Fig. 2(a) reasonably explained the SE results, a model consistent with sharp air/YIG and YIG/GGG interfaces was considered for the PKR data, which assumed the existence of the interface layers with zero MO activity (or zero magnetization). A reasonable agreement with the experimental spectra was achieved when a layer of zero magnetization (a magnetically dead layer) was inserted at the YIG/GGG interface, while the YIG at the air/YIG interface was left at bulk YIG MO activity. The optimal YIG/GGG interface layer thickness Δt varied between 1 nm and 2 nm and was found to be t-dependent and reach the lowest value in the thinnest film. The model assuming a magnetically dead interface layer was therefore rejected.

To eliminate the dependence on the penetration depth, finally, a model was employed with an YIG/GGG interface layer thickness Δt independent on the YIG film thickness but with an opposite sign of the YIG off-diagonal permittivity tensor element. The PKR spectra for the structure shown in Fig. 2(b) were computed for $\Delta t \approx 1.07$ nm which corresponds to the length of the body diagonal in an octant of the cubic YIG unit cell.[19] Using the YIG lattice constant (1.238 nm), one can estimate the length of the body diagonal to be $(3^{1/2}/2) \times 1.238\ \text{nm} = 1.07214$ nm. In Fig. 5, the experiment spectra are compared with those computed from the optical data for YIG and GGG materials assuming two models shown in Fig. 2. The model of Fig. 2(b) with the interface layer of the Fe^{3+} sublattice magnetization rotated by 180° with respect to the inner volume YIG demonstrates an improved agreement with the experiment. The effect of the interface layer is the strongest in the thinnest YIG film. This film also shows enhanced paraprocess probably due to a reduced Curie temperature.

The interpretation of the PKR spectra is based on the YIG ferrimagnetism.[19,24–27] The model in Fig. 2(a) assumes an YIG film of uniform distribution of Fe^{3+} sublattice magnetization, with the dominating tetrahedral sublattice magnetization parallel to the applied magnetic field. The model in Fig. 2(b) considers an interface layer with the opposite orientation of Fe^{3+} sublattice magnetization with respect to the rest of the film. In this layer, the Gd^{3+} sublattice magnetization and the octahedral Fe^{3+} sublattice magnetization are parallel to the applied magnetic field. The model takes into account antiferromagnetic exchange c-d coupling between Gd^{3+} in the dodecahedral sites (also called c sites) and Fe^{3+}

in the tetrahedral sites (also called *d* sites) across the interface.[28] Dominant contributions to the PKR spectra at $2\,\text{eV} < E < 4.5\,\text{eV}$ originate from the allowed transitions involving 3 d electrons of the strongly anti-ferromagnetically coupled $Fe^{3+}(d)$ and octahedral $Fe^{3+}(a)$ ions.[29] On this background, any $Gd^{3+}(c)$ structures originating from spin forbidden electronic *f-f* ($^8S_{7/2} \rightarrow {}^6P_{7/2}$, $^6P_{5/2}$, $^6P_{3/2}$, $^6I_{7/2}$) transitions in Gd^{3+} ($4f^7$, $^8S_{7/2}$) give too weak intensity to be detected.[30] Note that the normal reflectivity spectra of $Y_3Fe_5O_{12}$ and $Gd_3Fe_5O_{12}$ materials observed by Grant were nearly identical.[31] It is thus reasonable to take the interface layer MO contribution as that of YIG with reversed sign of PKR or with a reversed sign for the off-diagonal element of YIG permittivity tensor. The sign change of MO effects when the temperature going through a compensation point is a well-known phenomenon.[32–34]

As the films were subject to a post-deposition treatment at 800 °C, the moderate migration of Fe^{3+} from the YIG film and Ga^{3+} from the GGG substrate across the interface may take place. Using spin-wave resonance, Ramer and Wilts investigated surface effects in YIG films ($t \approx 500\,\text{nm}$) grown on GGG by chemical vapor deposition (CVD) before and after annealing in dry O_2 at 900 °C.[12] Their results provided the evidence for regions at the air/YIG and YIG/GGG interfaces with magnetic properties different from those of the bulk. In particular, the annealing produced an increase in the thickness of the YIG/GGG interface region. They explained the effect by the diffusion of Gd^{3+} and Ga^{3+} ions into YIG films which may produce layers with compensation points.[35–38]

Manuilov *et al*. conclude from their studies that in (111) YIG films grown by pulsed laser deposition ferric ions preferentially leave vacant octahedrally coordinated sites.[14] In gallium substituted iron garnets, in particular, $Y_3(FeGa)_5O_{12}$ and $Gd_3(FeGa)_5O_{12}$, the distribution of Fe^{3+} and Ga^{3+} ions among the tetrahedral and octahedral sites depends on the temperature and can be reversibly controlled by annealing at the temperatures from 800 to 1200 °C. The substitution of Fe^{3+} by Ga^{3+} preferentially involves the tetrahedral sites. It depends on the temperature and increases with defect concentration.[23]

A hypothetical $(Y_{1.5}Gd_{1.5})(FeGa)(Fe_{1.5}Ga_{1.5})O_{12}$ at the YIG/GGG interface as an ideal Néel ferrimagnet would have the magnetic moment of $8\,\mu_B$ (Bohr magneton) at 0 K and the Curie temperature around 200 K.[24,27] Its strong coupling to the inner volume YIG may preserve ferrimagnetic ordering above the room temperature with the magnetic moments of the $Gd^{3+}(c)$ and $Fe^{3+}(a)$ sublattices dominating that of the $Fe^{3+}(d)$ sublattice.[28,39] The fact that the obtained interface layer thickness only slightly exceeds the interface roughness (of several tenth of nanometer) indicates a very mild Fe^{3+} and Ga^{3+} migration across the YIG/GGG interface, which is consistent with the low defect concentration.[10,23]

Present work was devoted to the study of interface effects in nm-thick YIG films grown by sputtering and subject to a post-deposition heat treatment at 800 °C for 4 h. The films, distinguished by extremely low damping, were characterized using spectral ellipsometry and magneto-optical polar Kerr effect in the visible and near ultra-violet spectral region. The results confirm the high quality of YIG films with the properties converging to the bulk YIG materials. Both the ellipsometry and magneto-optic spectroscopic measurements indicate a nearly ideal air/YIG interface. The ellipsometry also predicts a nearly ideal YIG/GGG interface with negligible migration of Fe^{3+} and Ga^{3+} ions. On the other hand, the model for magnetooptics suggests the presence of a transition layer at the YIG/GGG interface that has Fe^{3+} sublattice magnetization opposite to that in the inner volume YIG due to antiferromagnetic coupling between $Gd^{3+}(c)$ and $Fe^{3+}(d)$ in the interface transition layer. The transition layer is restricted to the thickness of $\Delta t \approx 1\,\text{nm}$.

The work at Charles University was supported by Czech Science Foundation under Award 15-21547S. The work at Colorado State University was supported by the U.S. National Science Foundation under Award ECCS-1231598; the U.S. Army Research Office under Award W911NF-14-1-0501; the SHINES, an Energy Frontier Research Center funded by the U.S. Department of Energy, Office of Science, Basic Energy Sciences under Award SC0012670; and C-SPIN, one of the SRC STARnet Centers sponsored by MARCO and DARPA.

[1]Y. Sun, H. Chang, M. Kabatek, Y.-Y. Song, Z. Wang, M. Jantz, W. Schneider, M. Wu, E. Montoya, B. Kardasz, B. Heinrich, S. G. E. te Velthuis, H. Schultheiss, and A. Hoffmann, Phys. Rev. Lett. **111**, 106601 (2013).
[2]T. Liu, H. Chang, V. Vlaminck, Y. Sun, M. Kabatek, A. Hoffmann, L. Deng, and M. Wu, J. Appl. Phys. **115**, 17A501 (2014).
[3]O. d'Allivy Kelly, A. Anane, R. Bernard, J. B. Youssef, C. Hahn, A. H. Molpeceres, C. Carrétéro, E. Jacquet, C. Deranlot, P. Bortolotti, R. Lebourgeois, J.-C. Mage, G. de Loubens, O. Klein, V. Cros, and A. Fert, Appl. Phys. Lett. **103**, 082408 (2013).
[4]M. C. Onbasli, A. Kehlberger, D. H. Kim, G. Jakob, M. Kläui, A. V. Chumak, B. Hillebrands, and C. A. Ross, APL Mater. **2**, 106102 (2014).
[5]M. B. Jungfleisch, W. Zhang, W. Jiang, H. Chang, J. Sklenar, S. M. Wu, J. E. Pearson, A. Bhattacharya, J. B. Ketterson, M. Wu, and A. Hoffmann, J. Appl. Phys. **117**, 17D128 (2015).
[6]M. Haertinger, C. H. Back, J. Lotze, M. Weiler, S. Geprägs, H. Huebl, S. T. B. Goennenwein, and G. Woltersdorf, Phys. Rev. B **92**, 054437 (2015).
[7]M. Haidar, M. Ranjbar, M. Balinsky, R. K. Dumas, S. Khartsev, and J. Åkerman, J. Appl. Phys. **117**, 17D119 (2015).
[8]H. Chang, P. Li, W. Zhang, T. Liu, A. Hoffmann, L. Deng, and M. Wu, IEEE Magn. Lett. **5**, 6700104 (2014).
[9]E. Jakubisova-Liskova, S. Visnovsky, H. Chang, and M. Wu, J. Appl. Phys. **117**, 17B702 (2015).
[10]R. C. LeCraw, E. M. Gyorgy, and R. Wolfe, Appl. Phys. Lett. **24**, 573 (1974).
[11]C. H. Wilts and S. Prasad, IEEE Trans. Magn. **17**, 2405 (1981).
[12]O. G. Ramer and C. H. Wilts, Phys. Status Solidi B **79**, 313 (1977).
[13]R. Wolfe, J. C. North, R. L. Barns, M. Robinson, and H. J. Levinstein, Appl. Phys. Lett. **19**, 298 (1971).
[14]S. A. Manuilov, S. I. Khartsev, and A. M. Grishin, J. Appl. Phys. **106**, 123917 (2009).
[15]S. A. Manuilov and A. M. Grishin, J. Appl. Phys. **108**, 013902 (2010).
[16]S. A. Manuilov and P. A. Grünberg, J. Magn. Magn. Mater. **340**, 32 (2013).
[17]A. Mitra, O. Cespedes, M. Ali, and B. J. Hickey, see http://meetings.aps.org/link/BAPS.2015.MAR.B28.13 for APS March Meeting, #B28.013, 2015.
[18]D. L. Wood and K. Nassau, Appl. Opt. **29**, 3704 (1990).
[19]Y. Sun and M. Wu, *Solid State Physics: Recent Advances in Magnetic Insulators—From Spintronics to Microwave Applications*, edited by M. Wu, A. Hoffmann (Academic Press, Burlington, 2013), Vol. 64, p. 157–191.
[20]S. H. Wemple, S. L. Blank, J. A. Seman, and W. A. Biolsi, Phys. Rev. B **9**, 2134 (1974).
[21]Š. Višňovský, E. Lišková-Jakubisová, I. Harward, and Z. Celinski, Opt. Express **21**, 3400 (2013).

[22]D. E. Aspnes, J. B. Theeten, and F. Hottier, Phys. Rev. B **20**, 3292 (1979).
[23]P. Röschmann, J. Phys. Chem. Solids **42**, 337 (1981).
[24]S. Geller, H. J. Williams, G. P. Espinosa, and R. C. Sherwood, Bell Syst. Tech. J. **43**, 565 (1964).
[25]S. Geller, J. P. Remeika, R. C. Sherwood, H. J. Williams, and G. P. Espinosa, Phys. Rev. **137**, A1034 (1965).
[26]S. Geller, H. J. Williams, R. C. Sherwood, and G. P. Espinosa, J. Appl. Phys. **36**, 88 (1965).
[27]S. Geller, J. A. Cape, G. P. Espinosa, and D. H. Leslie, Phys. Rev. **148**, 522 (1966).
[28]E. L. Boyd, V. L. Moruzzi, and J. S. Smart, J. Appl. Phys. **34**, 3049 (1963).
[29]G. S. Krinchik, A. P. Khrebtov, A. A. Askochenskii, E. M. Speranskaya, and S. A. Belyaev, Sov. Phys. JETP **45**, 366 (1977).
[30]J. B. Gruber, M. E. Hills, C. A. Morrison, G. A. Turner, and M. R. Kokta, Phys. Rev. B **37**, 8564 (1988).
[31]P. M. Grant, Appl. Phys. Lett. **11**, 166 (1967).
[32]G. S. Krinchik and M. V. Chetkin, Sov. Phys. JETP **13**, 509 (1961).
[33]R. R. Alfano and D. H. Baird, Appl. Phys. Lett. **8**, 338 (1966).
[34]M. V. Chetkin and A. N. Shalygin, J. Appl. Phys. **39**, 561 (1968).
[35]K. P. Belov and A. V. Ped'ko, Sov. Phys. JETP **12**, 666 (1961).
[36]A. V. Ped'ko, Sov. Phys. JETP **14**, 505 (1962).
[37]J. P. Hanton and A. H. Morrish, J. Appl. Phys. **36**, 1007 (1965).
[38]B. Lüthi, Phys. Rev. **148**, 519 (1966).
[39]J. D. Litster and G. B. Benedek, J. Appl. Phys. **37**, 1320 (1966).